RESEARCH ARTICLE

Host–parasite interaction and microbiome response: effects of fungal infections on the bacterial community of the Alpine lichen *Solorina crocea*

Martin Grube[1], Martina Köberl[2], Stefan Lackner[2], Christian Berg[1] & Gabriele Berg[2]

[1]Institute of Plant Sciences, Karl-Franzens-University, Graz, Austria; and [2]Institute of Environmental Biotechnology, Graz University of Technology, Graz, Austria

Correspondence: Martin Grube, Institute of Plant Sciences, Karl-Franzens-University, Holteigasse 6, 8010 Graz, Austria. Tel.: +43 316 380 5655; fax: +43 316 380 9883; e-mail: martin.grube@uni-graz.at

Received 16 December 2011; revised 26 April 2012; accepted 25 May 2012.
Final version published online 3 July 2012.

DOI: 10.1111/j.1574-6941.2012.01425.x

Editor: Nina Gunde-Cimerman

Keywords
lichen symbiosis; host–parasite interaction; lichenicolous; microbiomes; pyrosequencing.

Abstract

The lichen symbiosis allows a self-sustained life under harsh environmental conditions, yet symbiotic integrity can be affected by fungal parasites. Nothing is known about the impact of these biologically diverse and often specific infections on the recently detected bacterial community in lichens. To address this question, we studied the arctic–alpine 'chocolate chip lichen' *Solorina crocea*, which is frequently infected by *Rhagadostoma lichenicola*. We sampled healthy and infected lichens at two different sites in the Eastern Alps. High abundances of *Acidobacteria, Planctomycetes,* and *Proteobacteria* were identified analyzing 16S rRNA gene regions obtained by barcoded pyrosequencing. At the phylum and genus level, no significant alterations were present among infected and healthy individuals. Yet, evidence for a differentiation of communities emerged, when data were analyzed at the strain level by detrended correspondence analysis. Further, a profile clustering network revealed strain-specific abundance shifts among *Acidobacteria* and other bacteria. Study of stability and change in host-associated bacterial communities requires a fine-grained analysis at strain level. No correlation with the infection was found by analysis of *nifH* genes responsible for nitrogen fixation.

Introduction

Lichen-forming fungi develop long-living thallus structures, which contain the symbiotic photoautotrophic algal partners in a mycelial shelter. The light-exposed joint organisms can be extremely robust to changing conditions in harsh natural environments. In these habitats, however, infections with specialized fungal parasites commonly occur. These lichen-inhabiting fungi have been recognized even before the nature of lichens was discovered to represent a fungal–algal symbiosis. Lichenicolous (= lichen-inhabiting) fungi are both taxonomically and biologically heterogeneous. Today more than 1800 species of lichenicolous fungi have been classified, but numerous lichenicolous fungi are still undescribed or recognized at species level (Lawrey & Diederich, 2003). The lifestyles of lichenicolous fungi range from parasitism to commensalism, and for some pathogens, preferences were shown for either the algal or fungal organism of the host symbiosis (Grube & Hafellner, 1990; De los Rios & Grube, 2000; Grube & de los Rios, 2001). Only few species progressively destroy the fungal structures of the lichens, whereas mild or localized infections are far more common. Interestingly, most of the species expressing mild infections and commensalic lifestyles are also highly specialized for their hosts. They form their reproductive structures only on their genuine host lichens.

Recent studies revealed the abundance of lichen-associated bacterial communities, which are now characterized in detail in their taxonomic and morphological structure (Cardinale *et al.*, 2006, 2008). All studies so far found evidence for host-specific bacterial communities (Grube *et al.*, 2009; Bates *et al.*, 2011; Hodkinson *et al.*, 2012). Yet, recent analyses also reveal effects of habitat parameters (Cardinale *et al.*, 2012), photobiont type, geography (Hodkinson *et al.*, 2012), and age of the thallus (Mushegian *et al.*, 2011; Cardinale *et al.*, 2012) on the composition of the bacterial communities. Fluorescent *in*

FEMS MICROBIOLOGY ECOLOGY

situ hybridization combined with confocal laser scanning microscopy suggests a general predominance of Alphaproteobacteria in growing parts of lichens (Cardinale *et al.*, 2012), whereas other bacterial phyla may become more prevalent in older parts. The aging of a lichen thallus is apparent in microscopic sections by decreased vitality of algae and morphological changes, such as in fine structure. Similar effects are sometimes also observed in parts of lichen thalli that are parasitized by lichenicolous fungi. We hypothesized a response of the bacterial community as a consequence to the fungal infection.

The effect of a lichenicolous fungal infection on the lichen microbiome was studied with the common and widespread soil-inhabiting lichen *Solorina crocea* (L.) Ach., also known as chocolate chip lichen (Fig. 1). It is a characteristic species of late snowbeds and found on acidic soils in arctic–alpine habitat above the tree line. The thalli are unique and easy to recognize by the crystallized bright red pigment (solorinic acid) produced on the lower surface. The vernacular name chocolate chip lichen refers to the large brownish fruitbodies (ascomata), which recall the color and appearance of chocolate. *Solorina crocea* is frequently infested by the lichenicolous fungus *Rhagadostoma lichenicola* (de Not.) Keissl. (*Sordariomycetes, Ascomycota*). As a specialized biotroph of *S. crocea*, this parasite develops crowded blackish ascomata on the upper surface of host thallus (see Fig. 1) and a richly branched, dark mycelium below the fruitbodies. The mycelium extends unspecifically and locally in the functional layers of the nearby lichen thallus. No specific infection structures are formed with algal or fungal host cells (M. Grube, unpublished observations). The infections persist on the thalli, yet fertility of the lichen is apparently not affected by the lichenicolous fungus. We used a barcoded pyrosequencing approach with different primers combined with a statistical design to analyze the bacterial community associated with healthy and infected lichens from two different sites in the Eastern Alps.

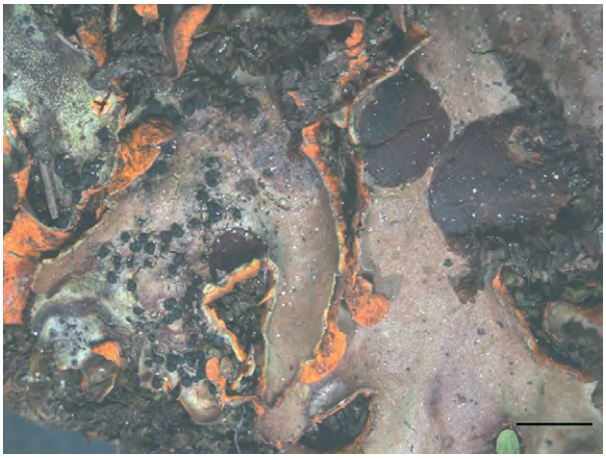

Fig. 1. The chocolate chip lichen *Solorina crocea* and its parasite *Rhagadostoma lichenicola* (black dots in right half of the image represent fruitbodies of the parasite). Zirbitzkogel (Image: W. Obermayer). Bar = 0.5 mm.

Materials and methods

Experimental design and sampling procedure

Lichen samples of *S. crocea* were collected in June 2011 from two different sampling points in the Austrian district Styria: Wölzer Tauern (N47°16.212, E14°22.860, 1892 m) and Zirbitzkogel, Ochsenboden (N47°4.65, E14° 33.783, 2050 m). At each site, three independent composite samples of five thalli were collected from healthy lichens and three from lichens, which were infested with the pathogenic fungus *R. lichenicola*. The typical fruitbodies of the fungal pathogen were detected by visual inspection using a 10× hand lens in the field and then confirmed using a stereomicroscope (Leica, Wetzlar, Germany). Because infections with this fungus occur locally on lobes of the host thalli, we sampled only thalli where multiple lobes were affected by the pathogen.

Total community DNA isolation

Total community DNA isolation was carried out with 2 g of each lichen sample. Samples were washed for 3 min with sterile 0.85% NaCl. The lichens were transferred into whirl packs and homogenized with 2 mL of 0.85% NaCl using mortar and pestle. From the liquid parts, 2 mL was centrifuged at high speed (16 000 ***g***, 4 °C) for 20 min, and resulting microbial pellets were stored at −70 °C. Total community DNA was extracted using the FastDNA® SPIN Kit for Soil (MP Biomedicals, Solon) according to the manufacturer's protocol. Resulting DNA concentrations ranged from 130.4 to 279.0 ng μL^{-1}. Metagenomic DNA samples were encoded using abbreviations indicating: (1) sampling location (W = Wölzer Tauern; Z = Zirbitzkogel), (2) independent replicate (W: A–F; Z: 1–3), and (3) status of infestation with the lichen pathogenic fungus *R. lichenicola* (healthy or infested).

Bacterial community analysis by 454 pyrosequencing of 16S rRNA genes

For the deep sequencing analysis of the lichen-associated bacterial community, the hypervariable V4-V5 region of the 16S rRNA gene (*Escherichia coli* positions 515–902) was amplified for pyrosequencing (Binladen *et al.*, 2007) using the primers Unibac-II-515f (Zachow *et al.*, 2008)

and 902R (Hodkinson & Lutzoni, 2009), containing the 454 pyrosequencing adaptors, linkers, and sample-specific tags (Table 1). The reverse primer 902R was specifically designed by Hodkinson & Lutzoni (2009) to target bacteria, but exclude sequences derived from lichen photobionts (chloroplasts of algae and *Cyanobacteria*). The PCR was performed using a total volume of 30 μL containing 1× Taq&Go (MP Biomedicals, Eschwege, Germany), 1.5 mM of $MgCl_2$, 0.2 μM of each primer, and 1 μL of template DNA (95 °C, 2 min; 35 cycles of 95 °C, 20 s; 64 °C, 15 s; 72 °C, 24 s; and elongation at 72 °C, 10 min). PCR products of two independent PCRs were pooled and purified by employing the Wizard® SV Gel and PCR Clean-Up System (Promega, Madison). Pyrosequencing libraries were generated by GATC Biotech (Konstanz, Germany) using the Roche 454 GS-FLX+ Titanium™ sequencing platform.

A taxonomy-based analysis was carried out with the web server SnoWMAn 1.11 (http://snowman.genome.tugraz.at). Primer sequences were cropped, and sequences shorter than 200 bp in length or of low quality (quality threshold 20) were removed from the pyrosequencing-derived data sets. The following SnoWMAn settings were used: analysis type: BLAT pipeline; reference database: greengenes_24-Mar-2010; rarefaction method: mothur; taxonomy: ribosomal database project (RDP); confidence threshold: 80%; include taxa covering more than: 1%. All analyses were performed with normalized data, considering the same number of sequences to all samples (1213 sequences per sample). For the normalization, strawberry perl 5.12.3.0 (http://strawberryperl.com) and the Perl program selector of the PANGEA pipeline (Giongo *et al.*, 2010) were used. To determine rarefaction curves, operational taxonomic units (OTUs) were identified at sequence divergences of 3% (species level), 5% (genus level), and 20% (phylum level) (Schloss & Handelsman, 2006; Will *et al.*, 2010), and curves were calculated using the tools aligner, complete linkage clustering, and rarefaction of the RDP pyrosequencing pipeline (http://pyro.cme.msu.edu) (Cole *et al.*, 2009). Shannon diversity (Shannon, 1997) and Chao1 richness (Chao & Bunge, 2002) indices were calculated based on the complete linkage clustering data.

Functional gene analysis by 454 pyrosequencing of *nifH* genes

Because fixation of atmospheric nitrogen is known as a key function in symbioses, we selected to analyze variation of nitrogenase genes as a functional marker. Nitrogenase genes are present in cyanobacteria, which commonly occur in the analyzed lichen species as a second autotrophic partner. The nitrogenase gene *nifH* was amplified according to a nested PCR protocol with primers designed by Zani *et al.* (2000). The reaction mixture of the first PCR (20 μL) was composed of 1× Taq&Go, 4 mM $MgCl_2$, 2 μM of the primers nifH4 and nifH3 (Zani *et al.*, 2000), and 1 μL of template DNA (95 °C, 5 min; 30 cycles of 95 °C, 1 min; 55 °C, 1 min; 72 °C, 1 min; and elongation at 72 °C, 10 min). Amplicons served as templates for the second PCR (30 μL) with the primer pair nifH1 and nifH2 designed by Zehr & McReynolds (1989), which contained the 454 pyrosequencing adaptors, linkers, and sample-specific tags (Table 1). Therefore, 3 μL of DNA was added to 1× Taq&Go, 1.5 mM $MgCl_2$, and 0.2 μM of each primer (95 °C, 5 min; 30 cycles of 95 °C, 1 min; 55 °C, 1 min; 72 °C, 1 min; and elongation at 72 °C, 10 min). Obtained PCR products of the independent replicates were pooled to one healthy and one infested composite sample per location and purified using Wizard® SV Gel and PCR Clean-Up System. Pyrosequencing libraries were created by

Table 1. Custom primers including 454 pyrosequencing adaptors (bold), linkers (italic), and sample-specific tags (underlined)

Name	Primer sequence	References
Unibac-II-515f_MID13	**CGTATCGCCTCCCTCGCGCCA***TCAG*CATAGTAGTGGTGCCAGCAGCCGC	
Unibac-II-515f_MID14	**CGTATCGCCTCCCTCGCGCCA***TCAG*CGAGAGATACGTGCCAGCAGCCGC	
Unibac-II-515f_MID29	**CGTATCGCCTCCCTCGCGCCA***TCAG*ACTGTACAGTGTGCCAGCAGCCGC	
Unibac-II-515f_MID30	**CGTATCGCCTCCCTCGCGCCA***TCAG*AGACTATACTGTGCCAGCAGCCGC	
Unibac-II-515f_MID31	**CGTATCGCCTCCCTCGCGCCA***TCAG*AGCGTCGTCTGTGCCAGCAGCCGC	
Unibac-II-515f_MID59	**CGTATCGCCTCCCTCGCGCCA***TCAG*CGTACTCAGAGTGCCAGCAGCCGC	
Unibac-II-515f_MID61	**CGTATCGCCTCCCTCGCGCCA***TCAG*CTATAGCGTAGTGCCAGCAGCCGC	
Unibac-II-515f_MID62	**CGTATCGCCTCCCTCGCGCCA***TCAG*TACGTCATCAGTGCCAGCAGCCGC	Zachow *et al.* (2008)
902r_454	**CTATGCGCCTTGCCAGCCCGC***TCAG*GTCAATTCITTTGAGTTTYARYC	Hodkinson & Lutzoni (2009)
nifH1_MID23	**CGTATCGCCTCCCTCGCGCCA***TCAG*TACTCTCGTGTGYGAYCCNAARGCNGA	
nifH1_MID24	**CGTATCGCCTCCCTCGCGCCA***TCAG*TAGAGACGAGTGYGAYCCNAARGCNGA	
nifH1_MID25	**CGTATCGCCTCCCTCGCGCCA***TCAG*TCGTCGCTCGTGYGAYCCNAARGCNGA	
nifH1_MID26	**CGTATCGCCTCCCTCGCGCCA***TCAG*ACATACGCGTTGYGAYCCNAARGCNGA	Zehr & McReynolds (1989)
nifH2_454	**CTATGCGCCTTGCCAGCCCGC***TCAG*ADNGCCATCATYTCNCC	Zehr & McReynolds (1989)

GATC Biotech using the Roche 454 GS-FLX+ Titanium system.

Primer sequences were trimmed, amplicon sequences with low quality (average base quality score 20) or a read length shorter than 200 bp were removed, and remaining sequences were translated into their amino acid sequence using the tool FrameBot of RDP's FunGene Pipeline (http://fungene.cme.msu.edu/FunGenePipeline). All subsequent analyses were carried out on amino acid sequences, which were normalized to 7005 sequences per sample using again STRAWBERRY PERL 5.12.3.0 and the Perl program selector of the PANGEA pipeline (Giongo *et al.*, 2010). Amino acid sequences were aligned and clipped at the same alignment reference position (~ 60 amino acids) using CLUSTALX 2.1 (Larkin *et al.*, 2007). Farnelid *et al.* (2011) showed that fragments encompassing the 60 amino acids of the *nifH* gene starting directly downstream from the nifH1 primer provide estimates comparable to those obtained with the full-length fragment of 108 amino acids. OTUs were classified, and rarefaction curves were constructed based on the distance matrices of amino acid sequences at 0%, 4%, and 8% dissimilarity (Farnelid *et al.*, 2011) using the tools mcClust and rarefaction of RDP's FunGene Pipeline. Diversity indices were ascertained based on the clustering data (Shannon, 1997; Chao & Bunge, 2002). Representative sequences at 92% similarity were selected for the following phylogenetic analysis (Farnelid *et al.*, 2011), where clusters with < 10 sequences were not designated. Nearest relatives were retrieved using the search tool TBLASTN of the National Center for Biotechnology Information (NCBI) database (http://blast.ncbi.nlm.nih.gov) with an *E*-value cutoff of 0.001.

Detrended correspondence and profile network clustering analysis

Detrended correspondence analysis (DCA) was used to detect differences in bacterial communities in healthy and infected lichen at the strain level. For this analysis, we used CANOCO 4.5 for Windows (Lepš & Smilauer, 2003) and defined OTUs at a dissimilarity level of 3%. The profile network analysis was carried out with those OTUs that showed a cumulative read change ≥ 5 sequences between the states. Average values of OTU read numbers were calculated for healthy and infected states of the two localities in a Microsoft Excel spreadsheet. If the ratio of values for healthy and infected states exceeded 1.5, the OTUs were regarded as altered and assigned to the respective clusters (abundant in healthy or infected). We considered only those OTUs that showed the same pattern in both sampling sites. Visualization of the network was carried out in CYTOSCAPE 2.8.2 (http://www.cytoscape.org).

Results

Pyrosequencing-based 16S rRNA gene profiling of lichen-associated bacteria

Using primers excluding lichen photobionts such as Cyanobacteria and chloroplasts of algae (Hodkinson & Lutzoni, 2009), a deep sequencing study of the bacterial communities associated with healthy and *Rhagadostoma*-infected *S. crocea* has been employed. Between 3221 and 1213 quality sequences per sample with a read length of $\geq$ 200 bp were recovered, which were normalized to the lowest number of sequences to all samples. Of all quality sequences 88.2% could be classified below the domain level. The rarefaction analyses of the amplicon libraries are shown in Supporting Information. Comparisons of the rarefaction analyses with the number of OTUs estimated by the Chao1 index revealed that at phylum level, 69.6–96.0% of estimated richness was recovered (Table 2). The pyrosequencing efforts at genus and species level reached 49.3–80.9% and 46.3–61.8%, respectively. The computed Shannon indices of diversity (H') barely showed differences between samples. At a genetic distance of 3% (species level), Shannon values ranged from 4.22 to 4.86.

Taxonomic analysis (Fig. 2) revealed that all samples of *S. crocea* were dominated by the bacterial phylum *Acidobacteria* (between 42.4% and 66.4% of sequences). Further dominant phyla present in all samples were *Planctomycetes* (7.2–25.2%) and *Proteobacteria* (11.1–30.0%). In lower concentrations but also found in all samples were lichen-associated *Actinobacteria* (1.3–5.2%). Considering only phyla covering more than 1% of quality sequences, *Bacteroidetes* were only detectable in one of the infested samples from Wölzer Tauern (2.0%). Most *Acidobacteria* reads were affiliated with subdivision 1 (93% of classified *Acidobacteria*), 6% were identified as belonging to subdivision 3. *Planctomycetes* sequences were classified as genera *Isosphaera* and *Gemmata* (46% and 34% of classified *Planctomycetes*). Among the *Proteobacteria*, only 19% could be identified to the genus level. *Sphingomonas* and *Novosphingobium* (*Alpha*-) as well as *Dyella* (*Gamma*-) and *Byssovorax* (*Deltaproteobacteria*) were found. The classifiable *Actinobacteria* (only 6%) were identified as *Nakamurella*. From both sampling locations together, infested metagenomes included nine genera, whereas healthy lichens harbored only seven of them. *Dyella* and *Nakamurella* occurred only in some samples infested with the lichen pathogen.

Pyrosequencing-based *nifH* profiling of lichen-associated communities

To analyze whether the fungal infection could have an effect on a key functional gene in the *S. crocea* symbiosis,

Table 2. Richness estimates and diversity indices for 16S rRNA gene and *nifH* gene amplicon libraries of *Solorina crocea* samples

	Quality sequences	Shannon index* (*H'*)			Rarefaction† (no. of OTUs)			Chao1‡ (no. of OTUs)			Coverage (%)		
16S rRNA gene													
Genetic dissimilarity		3%	5%	20%	3%	5%	20%	3%	5%	20%	3%	5%	20%
W_A-healthy	1213	4.22	3.76	1.62	261	190	36	528	336	45	49.5	56.6	80.0
W_F-healthy	1213	4.79	4.25	1.83	311	201	31	504	248	34	61.8	80.9	92.5
W_D-infested	1213	4.86	4.42	2.25	316	234	40	598	372	42	52.8	63.0	96.0
W_E-infested	1213	4.71	4.23	1.72	322	238	38	553	399	47	58.3	59.7	80.6
Z_1-healthy	1213	4.48	4.06	1.99	312	230	40	646	391	55	48.3	58.9	72.7
Z_3-healthy	1213	4.75	4.24	1.96	315	223	42	566	375	60	55.7	59.5	69.6
Z_2-infested	1213	4.78	4.16	1.63	294	206	47	488	372	64	60.2	55.3	73.4
Z_3-infested	1213	4.68	4.06	1.58	275	189	29	593	383	34	46.3	49.3	84.7
nifH gene													
Genetic dissimilarity		0%	4%	8%	0%	4%	8%	0%	4%	8%	0%	4%	8%
W_healthy	7005	3.53	3.06	2.16	1102	400	151	3853	658	285	28.6	60.8	52.9
W_infested	7005	2.78	2.41	1.80	831	310	123	3990	584	266	20.8	53.1	46.3
Z_healthy	7005	3.88	3.37	2.39	1259	432	181	5368	763	348	23.5	56.6	52.0
Z_infested	7005	3.92	3.24	2.55	1298	435	180	4067	782	355	31.9	55.6	50.7

*A higher number indicates more diversity.

†Results from the rarefaction analyses are also depicted in the Supporting Information.

‡Nonparametric richness estimator based on the distribution of singletons and doubletons.

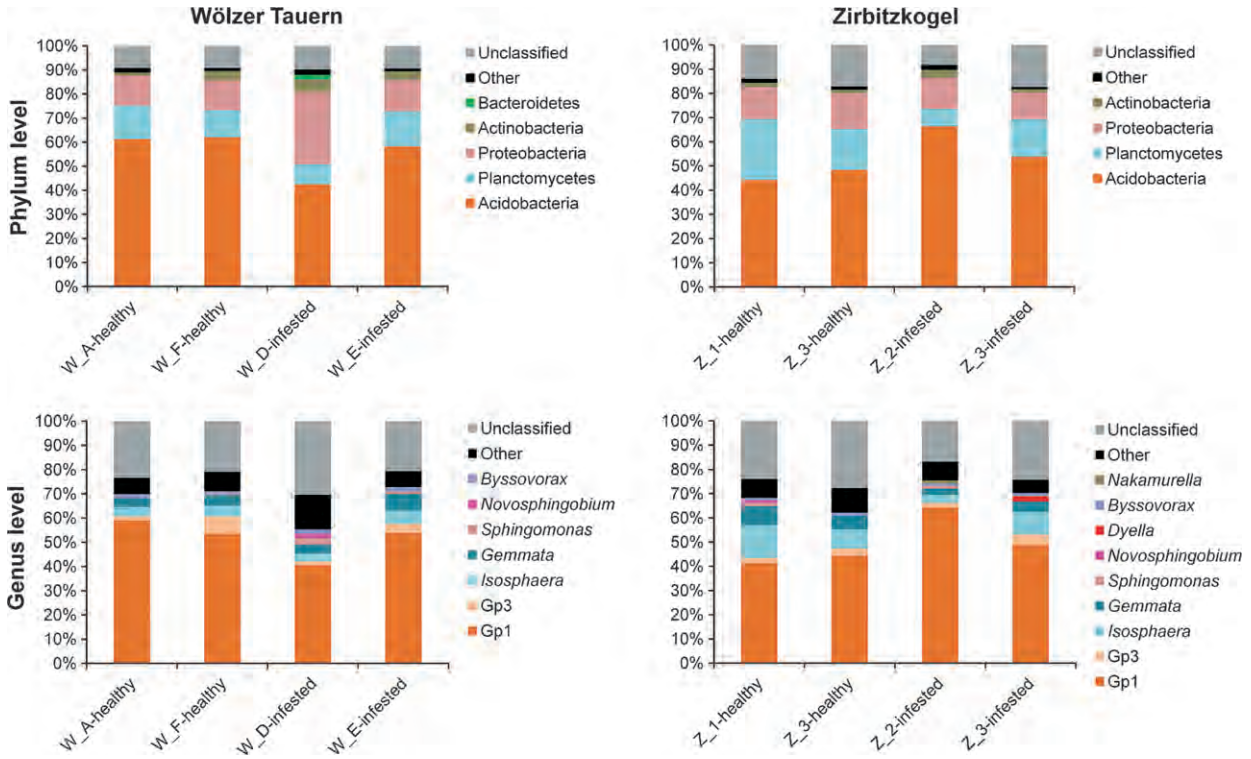

Fig. 2. Nonphotobiont bacterial communities associated with healthy and infested *Solorina crocea* samples from Wölzer Tauern and Zirbitzkogel. Relative clone composition of major phyla and genera was determined by pyrosequencing of 16S rRNA gene from metagenomic DNA. Phylogenetic groups accounting for $\leq$ 1% of all quality sequences are summarized in the artificial group 'Others'.

PCR amplicons of a fragment of the *nifH* gene were deep sequenced by a pyrosequencing approach. The number of quality reads with a read length of $\geq$ 200 bp varied among samples from 7005 to 10 788. To allow comparisons of diversity and richness, samples were normalized to the same number of sequences. The amino acid

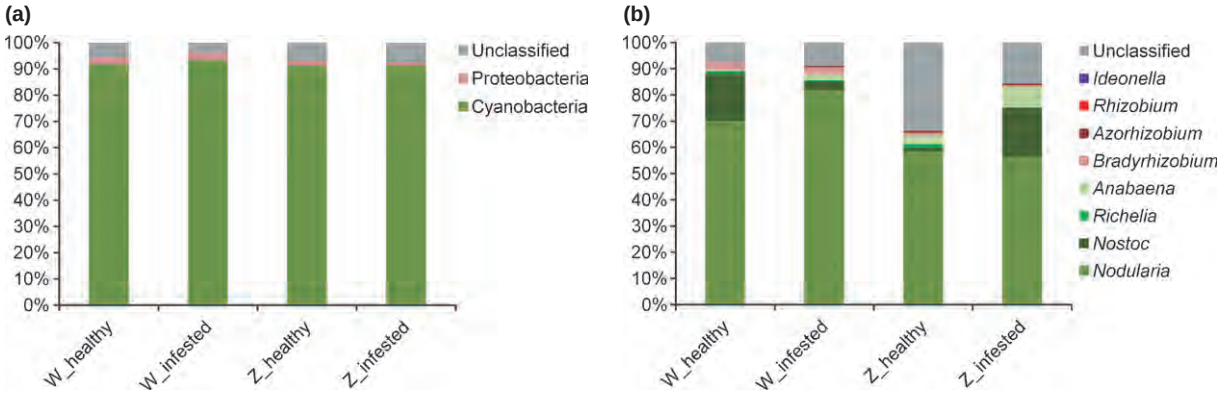

Fig. 3. Taxonomic classification of *nifH* gene communities associated with healthy and infested *Solorina crocea* samples from Wölzer Tauern and Zirbitzkogel. Amino acid sequences of the *nifH* genes were classified at phylum (a) and genus (b) level. Clusters containing < 10 sequences were not phylogenetically designated.

sequences were classified into 123–181 OTUs with a similarity cutoff of 92%. At this genetic similarity level, the coverage of Chao1 estimated richness reached 46.3–52.9% (Table 2). In general, Shannon indices (*H′*) were higher for *S. crocea* samples originating from Zirbitzkogel than for those from Wölzer Tauern. Three cutoff levels (100%, 96%, and 92% amino acid similarity) were used for generating rarefaction curves (Supporting Information).

Of all quality amino acid sequences, 94.1% could be classified to the phylum level. All classifiable sequences were affiliated to the canonical *nifH* cluster I (Chien & Zinder, 1996; Zehr *et al.*, 2003; Farnelid *et al.*, 2011), which includes mainly *Cyanobacteria, Alpha-*, *Beta-*, and *Gammaproteobacteria*. Not surprisingly for lichens, all samples showed an overwhelming dominance of *nifH* amplicons related to *Cyanobacteria* (between 91.2% and 93.2% of sequences) (Fig. 3). The noncyanobacterial diazotrophs were all assigned to *Proteobacteria* (between 1.3% and 3.1% of sequences). Most of the closest hits of cyanobacterial reads revealed the genus *Nodularia* (73%). Further, *Nostoc* (11%), *Anabaena* (4%), and *Richelia* (1%) were found. *Proteobacteria* sequences were classified as *Alpha-* (98%) and *Betaproteobacteria* (2%). Samples from Wölzer Tauern were dominated by *Bradyrhizobium*, whereas *Rhizobium* was found only in samples from Zirbitzkogel. *Ideonella* occurred only in the lichen pathogen-infested composite sample from Zirbitzkogel. However, we did not find a distinct community shift or depletion of cyanobacterial *nifH* genes with the infections.

DCA using CANOCO and profile clustering network analysis

Detrended correspondence analyses using presence/absence data of OTUs with a similarity cutoff of 97% indicate that strains are not randomly distributed in healthy and infected individuals of *S. crocea* (Fig. 4). The differences, however, are neither exclusive nor clear-cut. To gain better insight into the differences of healthy and infected lichens, we applied a profile clustering network analysis. This analysis revealed that several genetically distinct *Acidobacteria* are more abundant in infected samples (all belonging to *Acidobacteria* Gp 1) beside few *Proteobacteria*. *Bryocella elongata* and few other *Acidobacteria*,

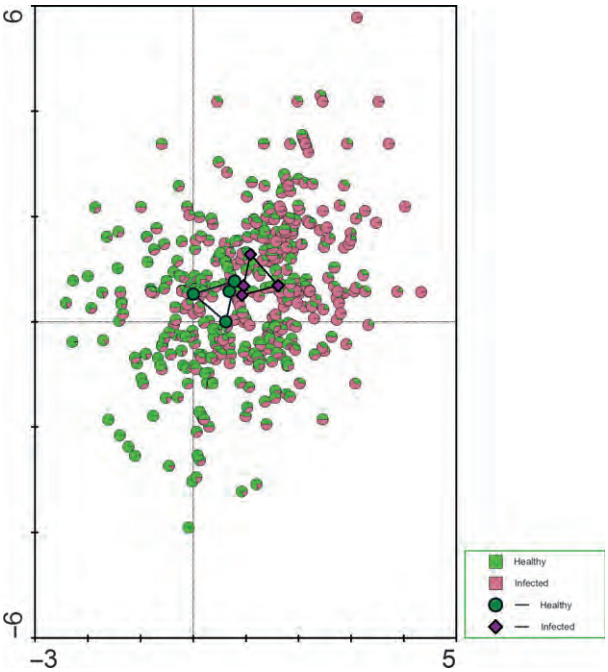

Fig. 4. DCA (indirect unimodal gradient analysis) of OTUs at a dissimilarity level of 3% identified by pyrosequencing. Eigenvalues of first and second axis are 0.325 and 0.150, respectively; sum of all eigenvalues 1.100. Diamonds show the location of the 8 samples and circles the location of the OTUs in the biplot. The colors indicate its preference to healthy (green) and/or infected (red) thalli of *Solorina*.

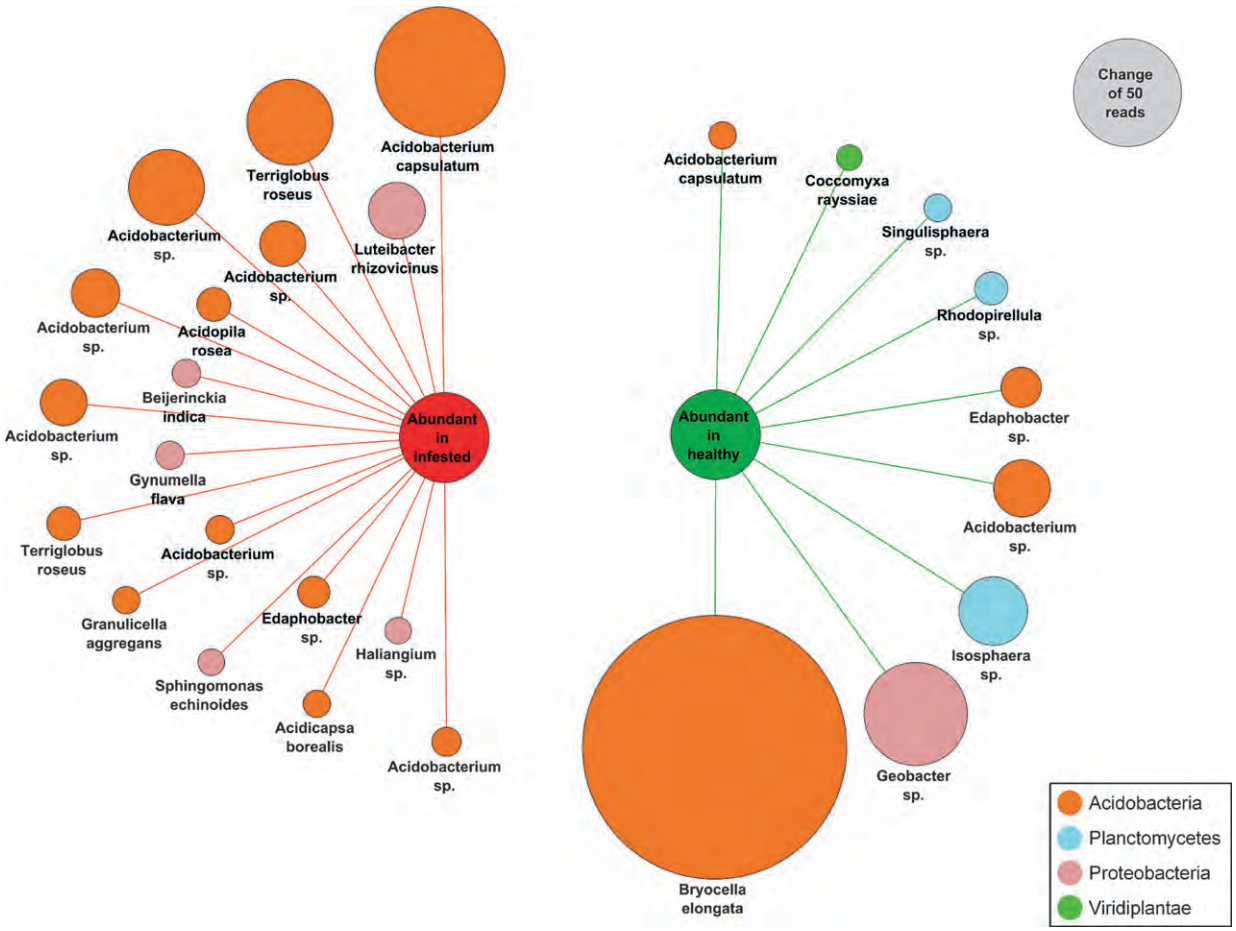

Fig. 5. Profile clustering network analysis of bacterial OTUs at a dissimilarity level of 3%. The relative abundance values for OTUs with a cumulative read change $\geq$ 5 were used; if the ratio of values for healthy and infected states exceeded 1.5 in one sampling site, the OTUs were regarded as altered and assigned to the respective clusters. Only those OTUs that featured the same pattern in both sampling sites are shown. Henceforth, each OTU is connected to either an 'abundant in infested' or 'abundant in healthy' node in the network. Node sizes of OTUs correspond to the mean relative abundance change between the states, and a node matching to a change of 50 reads was added as reference point.

strains of *Planctomycetes, Geobacter* (*Proteobacteria*), and the green-algal photobiont *Coccomyxa* appear more distinct in healthy individuals according to the network analysis (Fig. 5).

Discussion

Abundances of bacterial groups in host-associated microbiomes are often indicated as bar charts of phyla, classes, families, or genera. This approach is followed also in studies of lichen-associated microbiomes (Mushegian *et al.*, 2011; Hodkinson *et al.*, 2012). Evaluation at this level gives a general insight into microbial ecology of a microhabitat and agrees well with the notion of ecological coherence at high taxonomic ranks (Philippot *et al.*, 2011). At the phylum level, no clear differences were observed between the bacterial microbiomes of healthy thalli of *S. crocea* and those infected by the specific pathogenic fungus *R. lichenicola*. In both categories, we found a high proportion of *Acidobacteria* (which may exceed 50% of the sequence reads), as well as other bacterial groups such as *Planctomycetes* and *Proteobacteria*. Differences in the composition of bacteria at the genus level were likewise not clearly consistent with the lichenicolous infection status. Only the analysis of raw data revealed more genera in the infected samples, notably in the samples from Wölzer Tauern. This site has a slightly different habitat history than the Zirbitzkogel site. The wind-swept ridge of the Wölzer Tauern site represents a secondary habitat after nearby construction of wind power generators, whereas the Zirbitzkogel site was not affected by recent human activities. These differences, nevertheless, disappear when normalized data are used for the representation of microbiome composition. We were then

looking for possible differences between healthy and infected thalli at the lowermost taxonomic level and analyzed the sequence data as individual OTUs at a dissimilarity level of 3%, using DCA. In contrast to the results from analyses at higher taxonomic levels, we found that strains indeed segregate between healthy or infected samples (Fig. 4). Probably, because fungal-infected thalli also include to some extent externally healthy thallus material, these differences between healthy and infected thalli are not clear-cut. Using network analysis, we assessed which bacterial strains increase their occurrence in healthy or infected thalli. Interestingly, the recently described *Bryocella elongata* (Acidobacteria) appeared to be more typical for healthy thalli. *Bryocella elongata* was originally isolated from a methanotrophic enrichment culture obtained from an acidic *Sphagnum* peat (Dedysh *et al.*, 2012). A strain of *Acidobacterium capsulatum* was more frequent in infected thalli, yet a distinct strain of the same species occurred at slightly higher abundance in healthy lichens. Many others of these potential health-indicator strains could only be classified at the genus level because of insufficient information in public database for the time being. We suppose that these strains likely belong to yet-unculturable and new species of *Planctomycetes* and *Acidobacteria* (Fig. 5).

Our results suggest that the lichen-associated bacterial community reacts to infections of the host lichen by lichenicolous fungi by bacterial shifts at the strain level. Similar results are also found in other studies, for example, on bacterial communities affected by invasive bacteria (Jousset *et al.*, 2011).

The biology of many lineages in these large bacterial phyla *Planctomycetes* and *Acidobacteria* is still poorly understood, but their abundance in lichens and the strain-specific shifts indicate their fine-tuned ecological adaptation to the lichen habitat. The prevalence of *Acidobacteria* in our data set is somehow in contrast with the results of previous microscopic studies where *Alphaproteobacteria* were the prominent bacteria (Cardinale *et al.*, 2008; Grube *et al.*, 2009). These analyses focused mainly on young thallus parts, whereas in this study, we analyzed whole thalli, including the older parts. A recent study by us showed that old parts of thalli differed clearly in the composition with bacterial phyla (Cardinale *et al.*, 2012). A high number of *Acidobacteria* was recently also found in other analyses of lichen-associated microbiomes using whole thalli (Mushegian *et al.*, 2011; Hodkinson *et al.*, 2012). *Acidobacteria* of Gp1 made up a significantly higher proportion in central thallus parts of the rock-inhabiting *Xanthoparmelia* species (Mushegian *et al.*, 2011). The Gp1 lineage of *Acidobacteria* was also prevalent in our data set, irrespective of infection status. The second most abundant lineage of *Acidobacteria* in our data set was Gp3. *Acidobacteria* are well known as soil inhabitants, and their slow growth and tolerance to desiccation are ideal preconditions for a sustained presence in lichen thalli. We therefore argue that *Acidobacteria* are increasingly abundant in aging thallus parts.

At the genus level, the most important groups of the facultatively aerobic *Planctomycetes* were *Isosphaera* and *Gemmata*. The overall ecology of these genera is poorly known, but they are an ubiquitous, abundant aspect in acidic soils and bogs and may have particular mechanisms conferring tolerance to osmotic stress (Jenkins *et al.*, 2002), which is also a requirement to persist in the lichen habitat.

In agreement with the overall similarity of microbial communities at high taxonomic levels in healthy and infected thalli, we did not find a major shift in the phylogenetic spectrum of nitrogenase *nifH* genes, which is a key functional gene of this lichen symbiosis. Most reads belonged to cyanobacteria, which are known to be commonly present as a second autotrophic partner in *S. crocea*. However, closest BLAST hits of cyanobacterial *nifH* genes were with *Nodularia* and not with *Nostoc*, although the latter would be expected from microscopic studies (often seen as a layer below the algal layer in the thalli). A posteriori alignment of the data (not shown) revealed that the difference to the second closest hit (*Nostoc*) is only by one nonsynonymous mutation in the gene. In view of the abundance of *Nostoc* in the lichen thalli compared with the most abundant reads, we argue that the closest assignment to *Nodularia* is arbitrary, and in fact sequences are from *Nostoc*. We suggest that unreflected assignment of coding gene reads to genera, using only the first closest BLAST hits, could be a potential source of error, especially as we cannot exclude determination errors in the databases.

Lichens are a valuable system to study microbiome structure and variation. The light-exposed thalli can usually be regarded as well-delimited miniature ecosystems shaped by the name-giving lichenized fungal species (Grube *et al.*, 2009). We previously optimized analysis of these complex systems using a polyphasic approach (e.g. FISH and confocal laser scanning microscopy, fingerprinting: Cardinale *et al.*, 2008; Grube *et al.*, 2009). With the observation of shifts in lichen-associated bacterial communities at the strain level when exposed to biotic stress conditions, we conclude that functional dependencies in the lichen micro-ecosystem are finely tuned. It is known from other studies that related bacterial strains may differ in their effects on symbiotic relationships (e.g. Lehr *et al.*, 2007). *Rhagadostoma lichenicola* is a highly specific lichenicolous fungus, which relies on the function and integrity of the host thallus. The pathogen does not rapidly degrade the host and apparently persists on the hosts for

years. The observed subtle changes of the associated bacterial microbiome in infected thalli agree well with this ecology.

Acknowledgements

We greatly appreciated the financial support of the Austrian Science Foundation (FWF, I799 to MG and P19098 to GB). Sincere thanks to Walter Obermayer (Graz) for the image of *Solorina crocea*.

References

Bates ST, Cropsey GW, Caporaso JG, Knight R & Fierer N (2011) Bacterial communities associated with the lichen symbiosis. *Appl Environ Microbiol* **77**: 1309–1314.

Binladen J, Gilbert MT, Bollback JP, Panitz F, Bendixen C, Nielsen R & Willerslev E (2007) The use of coded PCR primers enables high-throughput sequencing of multiple homolog amplification products by 454 parallel sequencing. *PLoS ONE* **2**: e197.

Cardinale M, Puglia AM & Grube M (2006) Molecular analysis of lichen-associated bacterial communities. *FEMS Microbiol Ecol* **57**: 484–495.

Cardinale M, Vieira deCastroJ Jr, Müller H, Berg G & Grube M (2008) *In situ* analysis of the bacteria community associated with the reindeer lichen *Cladonia arbuscula* reveals predominance of *Alphaproteobacteria*. *FEMS Microbiol Ecol* **66**: 63–71.

Cardinale M, Steinová J, Rabensteiner J, Berg G & Grube M (2012) Age, sun and substrate: triggers of bacterial communities in lichens. *Environ Microbiol Rep* **4**: 23–28.

Chao A & Bunge J (2002) Estimating the number of species in a stochastic abundance model. *Biometrics* **58**: 531–539.

Chien YT & Zinder SH (1996) Cloning, functional organization, transcript studies, and phylogenetic analysis of the complete nitrogenase structural genes (nifHDK2) and associated genes in the archaeon *Methanosarcina barkeri* 227. *J Bacteriol* **178**: 143–148.

Cole JR, Wang Q, Cardenas E *et al.* (2009) The ribosomal database project: improved alignments and new tools for rRNA analysis. *Nucleic Acids Res* **37**: D141–D145.

De los Rios A & Grube M (2000) Host parasite interfaces of some lichenicolous fungi in the Dacampiaceae (Dothideales, Ascomycota). *Mycol Res* **104**: 1348–1353.

Dedysh SN, Kulichevskaya IS, Serkebaeva YM, Mityaeva MA, Sorokin VV, Suzina NE, Rijpstra WI & Damsté JS (2012) *Bryocella elongata* gen. nov., sp. nov., a member of subdivision 1 of the Acidobacteria isolated from a methanotrophic enrichment culture, and emended description of *Edaphobacter aggregans* Koch *et al.* 2008. *Int J Syst Evol Microbiol* **62**: 654–664.

Farnelid H, Andersson AF, Bertilsson S, Al-Soud WA, Hansen LH, Sørensen S, Steward GF, Hagström Å & Riemann L (2011) Nitrogenase gene amplicons from global marine surface waters are dominated by genes of non-cyanobacteria. *PLoS ONE* **6**: e19223.

Giongo A, Crabb DB, Davis-Richardson AG *et al.* (2010) PANGEA: pipeline for analysis of next generation amplicons. *ISME J* **4**: 852–861.

Grube M & de los Rios A (2001) Observations in *Biatoropsis usnearum* and other gall forming lichenicolous fungi using different microscopic techniques. *Mycol Res* **105**: 1116–1122.

Grube M & Hafellner J (1990) Studien an flechtenbewohnenden Pilzen der Sammelgattung *Didymella* (Ascomycetes, Dothideales). *Nova Hedwigia* **51**: 283–360.

Grube M, Cardinale M, de Castro JV Jr, Müller H & Berg G (2009) Species-specific structural and functional diversity of bacterial communities in lichen symbiosis. *ISME J* **3**: 1105–1115.

Hodkinson BP & Lutzoni F (2009) A microbiotic survey of lichen-associated bacteria reveals a new lineage from the Rhizobiales. *Symbiosis* **49**: 163–180.

Hodkinson BP, Gottel NR, Schadt CW & Lutzoni F (2012) Photoautotrophic symbiont and geography are major factors affecting highly structured and diverse bacterial communities in the lichen microbiome. *Environ Microbiol* **14**: 147–161.

Jenkins C, Kedar V & Fuerst JA (2002) Gene discovery within the planctomycete division of the domain Bacteria using sequence tags from genomic DNA libraries. *Genome Biol* **3**: RESEARCH0031.

Jousset A, Schulz W, Scheu S & Eisenhauer N (2011) Intraspecific genotypic richness and relatedness predict the invasibility of microbial communities. *ISME J* **5**: 1108–1114.

Larkin MA, Blackshields G, Brown NP *et al.* (2007) ClustalW and ClustalX version 2.0. *Bioinformatics* **23**: 2947–2948.

Lawrey JD & Diederich P (2003) Lichenicolous fungi: interactions, evolution, and biodiversity. *Bryologist* **106**: 81–120.

Lehr NA, Schrey SD, Bauer R, Hampp R & Tarkka MT (2007) Suppression of plant defence response by a mycorrhiza helper bacterium. *New Phytol* **174**: 892–903.

Lepš J & Smilauer P (2003) *Multivariate Analysis of Ecological Data Using Canoco*. Cambridge University Press, Cambridge.

Mushegian AA, Peterson CN, Baker CC & Pringle A (2011) Bacterial diversity across individual lichens. *Appl Environ Microbiol* **77**: 4249–4252.

Philippot L, Andersson SGE, Battin TJ, Prosser JI, Schimel JP, Whitman WB & Hallin S (2010) The ecological coherence of high bacterial taxonomic ranks. *Nat Rev Microbiol* **8**: 523–529.

Schloss PD & Handelsman J (2006) Toward a census of bacteria in soil. *PLoS Comput Biol* **2**: e92.

Shannon CE (1997) The mathematical theory of communication. 1963. *MD Comput* **14**: 306–317.

Will C, Thürmer A, Wollherr A, Nacke H, Herold N, Schrumpf M, Gutknecht J, Wubet T, Buscot F & Daniel R (2010) Horizon-specific bacterial community composition of German grassland soils, as revealed by

pyrosequencing-based analysis of 16S rRNA genes. *Appl Environ Micobiol* **76**: 6751–6759.

Zachow C, Tilcher R & Berg G (2008) Sugar beet-associated bacterial and fungal communities show a high indigenous antagonistic potential against plant pathogens. *Microb Ecol* **55**: 119–129.

Zani S, Mellon MT, Collier JL & Zehr JP (2000) Expression of *nifH* genes in natural microbial assemblages in Lake George, New York, detected by reverse transcriptase PCR. *Appl Environ Microbiol* **66**: 3119–3124.

Zehr JP & McReynolds LA (1989) Use of degenerate oligonucleotides for amplification of the *nifH* gene from the marine cyanobacterium *Trichodesmium thiebautii*. *Appl Environ Microbiol* **55**: 2522–2526.

Zehr JP, Jenkins BD, Short SM & Steward GF (2003) Nitrogenase gene diversity and microbial community structure: a cross-system comparison. *Environ Microbiol* **5**: 539–554.

Supporting Information

Additional Supporting Information may be found in the online version of this article:

Fig. S1. Rarefaction analyses for 16S rRNA gene amplicon libraries of *Solorina crocea* samples from Wölzer Tauern (a) and Zirbitzkogel (b).

Fig. S2. Rarefaction analyses for *nifH* sequence libraries of *Solorina crocea* samples.

Please note: Wiley-Blackwell is not responsible for the content or functionality of any supporting materials supplied by the authors. Any queries (other than missing material) should be directed to the corresponding author for the article.